Method for comparing visual field defects to local RNFL and RGC damage seen on frequency domain OCT in patients with glaucoma.

Donald C. Hood[1,2,*] and Ali S. Raza[1]

[1]*Department of Psychology, Columbia University, New York, NY. 10027, USA*
[2]*Department of Ophthalmology, Columbia University, New York, NY. 10027, USA*
**dch3@columbia.edu*

Abstract: To relate structural (anatomical) and functional (behavioral) measures of glaucomatous damage, a method is described for comparing visual field defects to local retinal ganglion cell (RGC) and retinal nerve fiber layer (RNFL) thicknesses. Thickness maps of the RNFL and the RGC + inner plexiform layer, obtained with frequency domain optical coherence tomography (fdOCT), were transformed into probability maps by comparing them to a normative group. As demonstrated in patients with glaucomatous damage to the macula, the probability map associated with the patient's visual field can be directly compared to the fdOCT probability maps by taking into consideration the displacement of the RGCs.

OCIS codes: (170.4500) Optical coherence tomography; (330.4300) Vision system - noninvasive assessment; (170.4470) Ophthalmology

References and links

1. D. Huang, E. A. Swanson, C. P. Lin, J. S. Schuman, W. G. Stinson, W. Chang, M. R. Hee, T. Flotte, K. Gregory, C. A. Puliafito, and J. G. Fujimoto, "Optical coherence tomography," Science **254**(5035), 1178–1181 (1991).
2. J. S. Schuman, M. R. Hee, A. V. Arya, T. Pedut-Kloizman, C. A. Puliafito, J. G. Fujimoto, and E. A. Swanson, "Optical coherence tomography: a new tool for glaucoma diagnosis," Curr. Opin. Ophthalmol. **6**(2), 89–95 (1995).
3. M. Wang, D. C. Hood, J.-S. Cho, Q. Ghadiali, C. V. De Moraes, X. Zhang, R. Ritch, and J. M. Liebmann, "Measurement of local retinal ganglion cell layer thickness in patients with glaucoma using frequency-domain optical coherence tomography," Arch. Ophthalmol. **127**(7), 875–881 (2009).
4. O. Tan, V. Chopra, A. T. Lu, J. S. Schuman, H. Ishikawa, G. Wollstein, R. Varma, and D. Huang, "Detection of macular ganglion cell loss in glaucoma by Fourier-domain optical coherence tomography," Ophthalmology **116**(12), 2305–2314.e2, (2009).
5. A. S. Raza, J. Cho, C. G. V. De Moraes, M. Wang, X. Zhang, R. H. Kardon, J. M. Liebmann, R. Ritch, and D. C. Hood, "Macular retinal ganglion cell layer thickness and local visual field sensitivity in glaucoma," Arch. Ophthalmol. (to be published).
6. N. R. Kim, E. S. Lee, G. J. Seong, J. H. Kim, H. G. An, and C. Y. Kim, "Structure-function relationship and diagnostic value of macular ganglion cell complex measurement using Fourier-domain OCT in glaucoma," Invest. Ophthalmol. Vis. Sci. **51**(9), 4646–4651 (2010).
7. J. W. Cho, K. R. Sung, S. Lee, S. C. Yun, S. Y. Kang, J. Choi, J. H. Na, Y. Lee, and M. S. Kook, "Relationship between visual field sensitivity and macular ganglion cell complex thickness as measured by spectral-domain optical coherence tomography," Invest. Ophthalmol. Vis. Sci. **51**(12), 6401–6407 (2010).
8. D. C. Hood, A. S. Raza, C. G. V. de Moraes, J. G. Odel, V. C. Greenstein, J. M. Liebmann, and R. Ritch, "Initial arcuate defects within the central 10 degrees in glaucoma," Invest. Ophthalmol. Vis. Sci. **52**(2), 940–946 (2011).
9. Q. Yang, C. A. Reisman, Z. Wang, Y. Fukuma, M. Hangai, N. Yoshimura, A. Tomidokoro, M. Araie, A. S. Raza, D. C. Hood, and K. Chan, "Automated layer segmentation of macular OCT images using dual-scale gradient information," Opt. Express **18**(20), 21293–21307 (2010).
10. N. Drasdo, C. L. Millican, C. R. Katholi, and C. A. Curcio, "The length of Henle fibers in the human retina and a model of ganglion receptive field density in the visual field," Vision Res. **47**(22), 2901–2911 (2007).
11. D. C. Hood and V. C. Greenstein, "Multifocal VEP and ganglion cell damage: applications and limitations for the study of glaucoma," Prog. Retin. Eye Res. **22**(2), 201–251 (2003).

1. Introduction

Glaucoma is a progressive optic neuropathy that damages the retinal ganglion cells (RGC) and their axons. To diagnose and follow glaucoma, visual fields are typically obtained in addition

#143101 - $15.00 USD Received 25 Feb 2011; revised 28 Mar 2011; accepted 28 Mar 2011; published 5 Apr 2011

to fundus examinations. These visual fields, usually obtained with standard automated perimetry (SAP), have the advantage of providing a topographical spatial representation of the visual loss, which can be compared to characteristic patterns of glaucomatous loss. Today many clinicians augment this information with images from optical coherence tomography (OCT).

OCT is a non-invasive test that employs near-infrared light in much the same way that ultrasound uses sound [1,2]. With the newer frequency domain (fd) OCT, it is possible to measure the thickness of the two layers damaged by glaucoma, the retinal nerve fiber layer (RNFL), which contains the axons of the RGCs, and the RGC plus the inner plexiform layer (IPL), which contains the RGC bodies as well as the connections of the cells of the inner nuclear layer to these RGCs (e.g., [3–7]).

While numerous studies have documented the efficacy of the fdOCT in detecting glaucomatous damage, it is still not clear how best to combine fdOCT information with SAP visual field data. One can always ask whether each is normal or not, but this does not take advantage of the spatial information available on the fdOCT tests. For example, if the abnormal regions on both tests match, one would have more confidence in a diagnosis of glaucoma than if different regions were abnormal on each test. Our purpose here is to describe a method for comparing spatially local visual field defects to local RGC + IPL and RNFL thicknesses. We illustrate this method by applying it to patients with glaucomatous damage to the macula.

2. Methods

2.1. Subjects

Macular and disc 6mm x 6mm cube scans (Topcon, Inc, Paramus, NJ) were obtained from healthy controls and patients. The normative group (39 ± 14 yrs) consisted of 128 eyes from 128 controls (data supplied by Topcon, Inc.). To be included, subjects were required to have a correction between + 3.0D and −6.0D, IOP ≤ 21 mmHg, axial length between 22 and 26 mm, a normal clinical exam, and normal visual fields (SITA Standard, Carl Zeiss Meditec, Inc, Dublin, CA; reliability indices all ≤ 33%). Exclusion criteria included history of ocular disease or a family history of glaucoma. The patient group (58 ± 14 yrs) consisted of 16 eyes (12 patients) with glaucomatous optic neuropathy, based on a clinical fundus examination. All patients also underwent 24-2 and 10-2 visual field testing. They were selected from a larger group of patients based upon a normal 24-2 visual field outside the central 10° [8]. In particular, eyes were excluded if their 24-2 test had a cluster of 3 contiguous points (5%, 5%, 1%) within a hemifield, but outside the central 10°. The total deviation plots were used for all visual field analyzes.

Written informed consent was obtained from all subjects. Procedures followed the tenets of the Declaration of Helsinki, and the protocol was approved by the Committee of the Institutional Board of Research of Columbia University.

2.2. OCT analysis

Using an automated segmentation algorithm [9], three borders were defined: the vitreous/RNFL, RNFL/RGC, and IPL/inner nuclear layer borders (Fig. 1A). An experienced operator hand-corrected the automatic segmentation of the combined RGC and inner plexiform layers (RGC + IPL) of 128 horizontal B-scans for each cube scan. From these segmented lines, RNFL and RGC + IPL thicknesses were obtained as shown by the red (RGC + IPL) and green (RNFL) bars in Fig. 1. The thickness measures were then smoothed in two dimensions for the 6 by 6 mm (20° by 20°) area of interest with a two-dimensional averaging filter using a window size of about 80 μm. For each cube scan, thickness maps as in the left column of Fig. 1 were obtained. There were 3 such maps: macular RGC + IPL thickness, macular RNFL thickness, and optic disc RNFL thickness. The thicknesses corresponding to the pseudo-colors are shown on the calibration bars in this figure. Note that a RGC + IPL

#143101 - $15.00 USD Received 25 Feb 2011; revised 28 Mar 2011; accepted 28 Mar 2011; published 5 Apr 2011

thickness map also can be generated from the optic disc cube scan. However, given how thin the RGC layer is in this region, it does not add to the analysis.

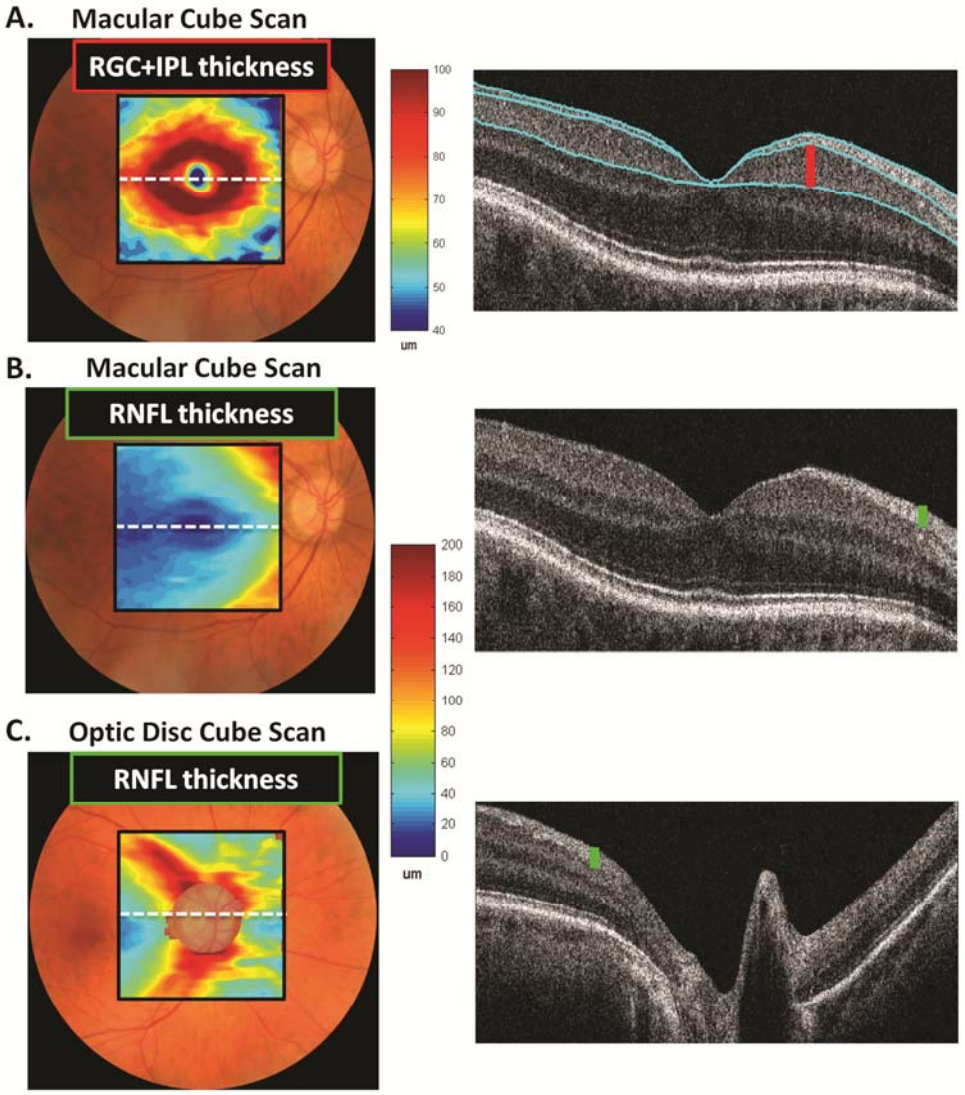

Fig. 1. Sample thickness maps and scans from a healthy control. A. RGC + IPL thickness map (left) and a scan through the horizontal meridian with the segmentation displayed in light blue (right). B. RNFL thickness map (left) and a scan through the horizontal meridian (right). C. RNFL thickness map (left) and a scan through the center of the optic disc (right).

3. Results

3.1. The method

Figure 1A (left panel) shows a pseudo-color representation of the RGC + IPL thickness of a healthy control based upon the macular cube scan. As expected, the greatest RGC + IPL thickness is just outside the foveal center at about 4°. By around 10°, the thickness is reaching an asymptotic level.

In contrast, the RNFL thickness derived from the same cube scan (Fig. 1B, left panel) shows a different pattern. As expected, the RNFL is relatively thin except in the arcuate

#143101 - $15.00 USD Received 25 Feb 2011; revised 28 Mar 2011; accepted 28 Mar 2011; published 5 Apr 2011

regions. A better picture of the arcuate RNFL can be seen in Fig. 1C (left panel), which depicts the thickness of the RNFL for the optic disc, cube scan. Because the macular and optic disc cube scans provide overlapping information about RNFL thickness, they were combined into one map as in Fig. 2A by co-registration based upon blood vessel alignment in an *en face* view of the fdOCT scan. The same maps are shown in Fig. 2B with iso-thickness contours added, while Fig. 2C shows the RGC + IPL map in the same format. Note that both maps were flipped across the horizontal axis so as to be presented in the same way as the visual field. Additionally, the results for left eyes were flipped across the vertical axis so that all eyes were presented as right eyes in all figures.

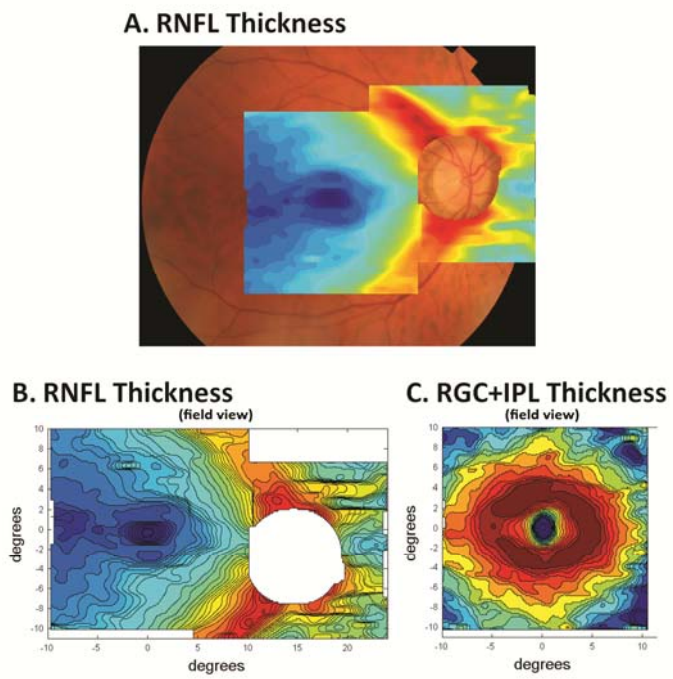

Fig. 2. RGC + IPL and RNFL thickness maps for the control in Fig. 1A. Combined RNFL thickness maps from scans of the macula and optic disc. B. Same scans as in A shown with iso-thickness contours and after flipping across the horizontal axis to present in field view. C. Same as in B for RGC + IPL thickness.

Figure 3A presents the 24-2 and 10-2 visual fields and the 3 thickness maps illustrated in Fig. 1 for the healthy control in Fig. 1. The red circles have a radius of 10°. Figures 3B-D show the results from 3 patients. (Note that in all figures, the OCT results are flipped along the horizontal axis to coincide with the field view.) Patients 1 and 2 have clear arcuate defects that can be seen on the 10-2 and all three OCT thickness maps. Patient 3's visual field damage is more subtle, although again there appears to be an indication of an upper field arcuate defect that appears to be confirmed on the OCT maps (red arrows). However, we cannot tell if the cluster of abnormal points on the visual field (green arrow) corresponds to the region that appears thinned (red arrows) in the OCT scans. In particular, is the RGC + IPL thinning in the same place as the abnormal points on the 10-2 (green arrow); and, does the OCT thinning reach statistical significance?

To address the first question, we need a way to relate the location of the visual field points to the region of the RGCs activated by these points. To make this comparison, we must take into consideration the displacement of the RGCs near the fovea. That is, light falling on receptors near the foveal center excite RGCs that are some distance from this location. As

#143101 - $15.00 USD Received 25 Feb 2011; revised 28 Mar 2011; accepted 28 Mar 2011; published 5 Apr 2011

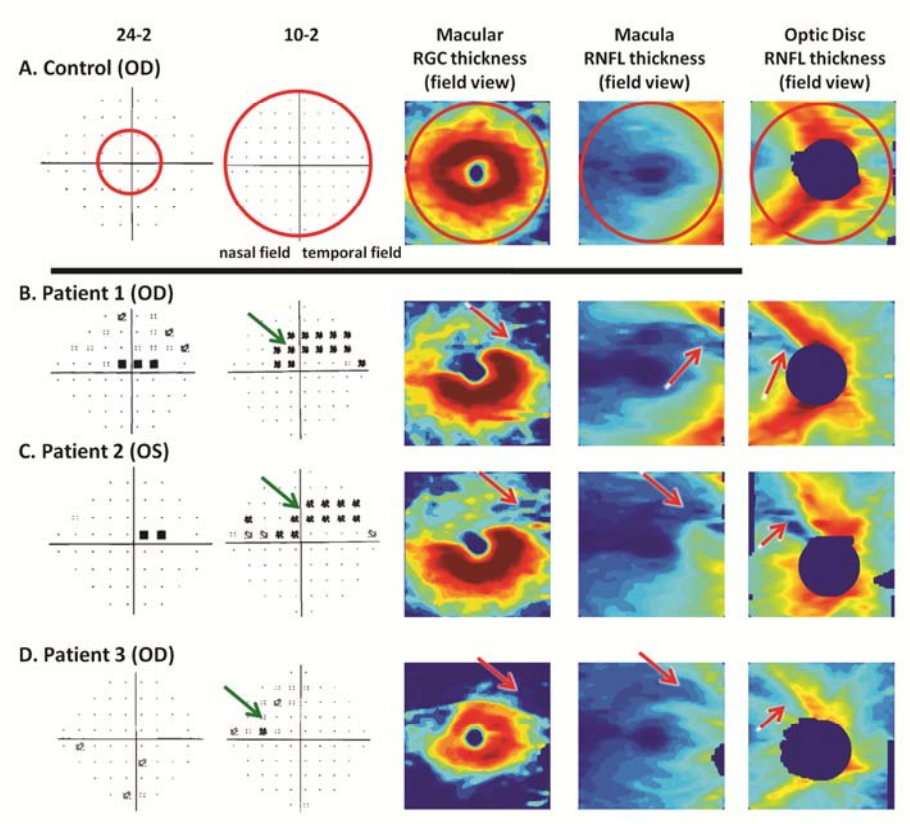

Fig. 3. Sample visual fields and OCT thickness maps. A. 24-2 (left panel) and 10-2 (second column) visual fields are shown for a healthy control along with the thickness maps for the macula RGC + IPL (middle panel) and RNFL thickness (fourth panel), and the optic disc RNFL thickness (right panel). B,C,D. Same as in A for 3 patients.

previously reported [5,8], we can use the results of Drasdo et al. [10] to locate the average location of the excited RGCs for each of the visual field points. Note, this does not take into consideration any variation in RGC displacement that may occur from one individual to another. Figure 4A shows the thickness maps for patient 1 presented as in Figs. 2B,C. In Fig. 4B, the superimposed small circles show the retinal location of the RGCs associated with the 10-2 (small circles) test locations.

To address the second question, the OCT thickness maps need to be transformed into probability maps. To do this, the local OCT thickness for an individual is compared to the distribution of thicknesses of the 128 healthy control eyes. The maps in Fig. 4C show the results as a continuous probability scale. This scale is shown in the middle of this panel, where dark green indicates a p value of greater than 10%, yellow 5%, red about 1% and dark red <1%.

The final step involves combining the probability information from the visual fields and the OCT images. Figure 5A shows the combined OCT/10-2 probability maps for patient 1. The significantly abnormal points from this patient's 10-2 visual field (Fig. 3B, second column) are shown as the yellow (5%) and red (<1%) circles. It is easy to see the agreement between the probability maps for the 10-2 and OCT thicknesses.

#143101 - $15.00 USD Received 25 Feb 2011; revised 28 Mar 2011; accepted 28 Mar 2011; published 5 Apr 2011

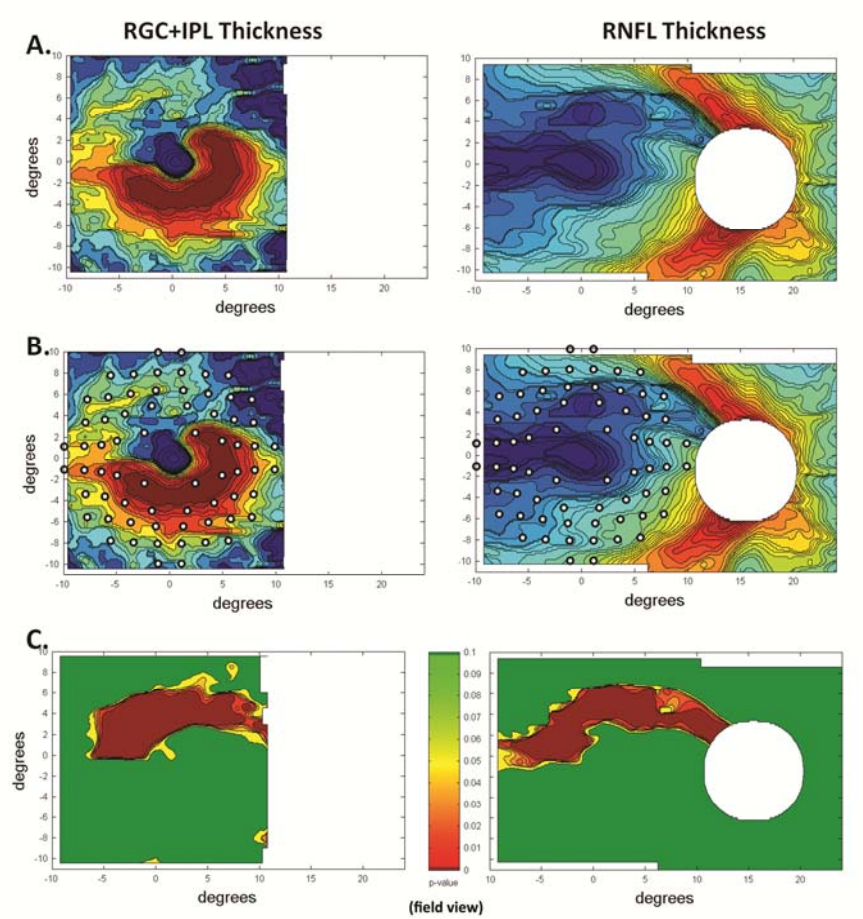

Fig. 4. RGC + IPL and RNFL maps for patient 1. A. OCT thickness maps as in Figs. 2B, C. B. Maps from panel A with 10-2 test locations displaced based upon displacement of RGCs. C. Probability maps for OCT thickness.

Figures 5B,C show the combined OCT/10-2 probability maps for the other 2 patients in Fig. 3. The combined probability maps (Fig. 5B) for patient 2 resemble those for patient 1. For patient 3, while the visual fields suggest that the damage is relatively confined and subtle, the RGC + IPL probability map suggests more extensive damage.

3.2. Patient data

The 10-2 visual fields of the 16 patient eyes were classified as arcuate or partial arcuate (8), diffuse (1), and normal (7). Figures 3B-D shows the field and OCT data for 3 of the 8 patients with arcuate or partial arcuate visual fields. The combined OCT/10-2 probability maps for these 3 patients are shown in Fig. 5. For all 8 arcuate visual fields, the RGC + IPL and RNFL probability maps showed arcuate damage in the same region in which the visual field contained abnormal points. In six cases, both the significantly abnormal portions of the OCT and fields coincided as seen for Patients 1 and 2 (Figs. 5A,B). In two eyes (same patient), the OCT abnormal region included both hemifields, while the visual field showed abnormalities only in the superior field (Fig. 5C). For the eye with the diffuse visual field, the OCT probability map showed damage in both hemispheres.

#143101 - $15.00 USD Received 25 Feb 2011; revised 28 Mar 2011; accepted 28 Mar 2011; published 5 Apr 2011

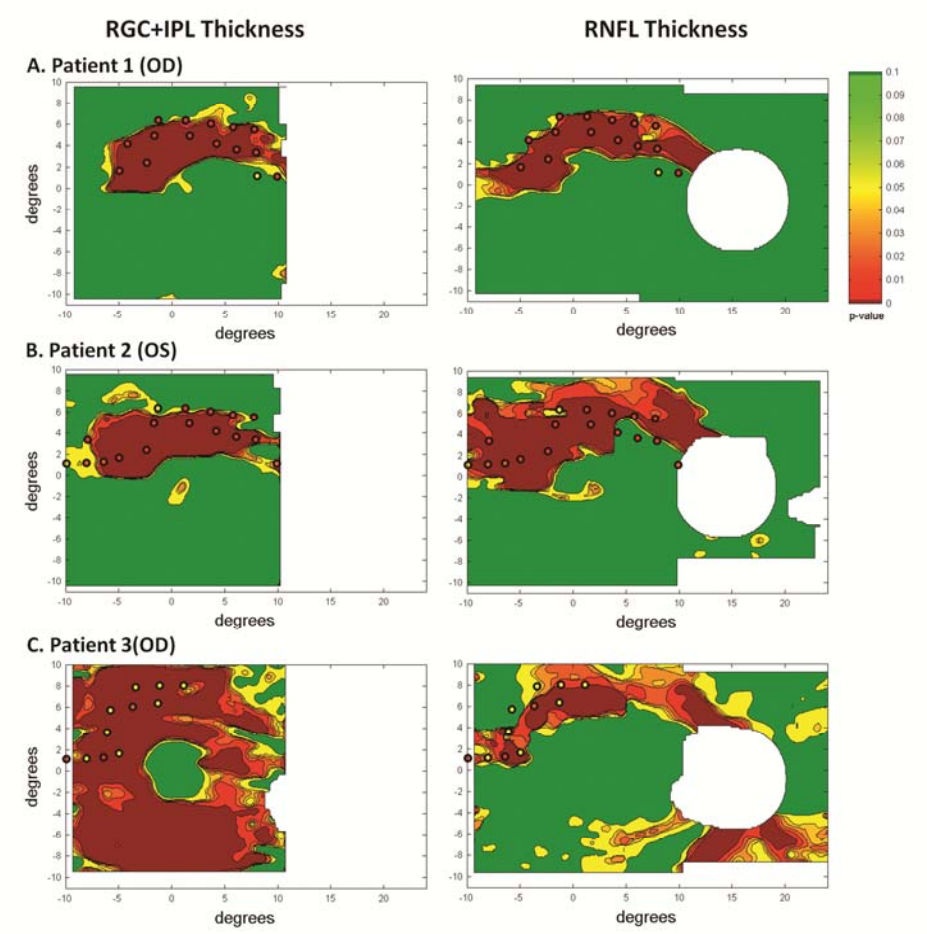

Fig. 5. A-C. Combined OCT/10-2 probability maps for the 3 patients from Fig. 3.

Five of the 7 eyes with 10-2 visual fields classified as normal had OCT probability maps within the normal range. The other 2 are of particular interest. In one case, Patient 4, there were abnormal points in the upper field of the 10-2 (Fig. 6C), although the visual field was normal based upon MD, PSD and cluster criteria. Of note is that the combined OCT/10-2 maps (Figs. 6A,B) showed evidence of an arcuate defect in both hemispheres. Figure 7 shows the results for Patient 5 (OD), the 7th eye with a normal visual field. Note the arcuate damage on the OCT corresponding to a lower field arcuate defect. The 10-2 Total Deviation plot did not show a single abnormal point (Fig. 7C). In fact, these points were nearly all positive (more sensitive than normal), as if this patient had a higher baseline sensitivity or lower criterion for saying "I see it". In any case, the Pattern Deviation map (Fig. 7D), although normal based upon MD and PSD criteria, showed significantly abnormal points in the region corresponding to the lower field arcuate seen on the OCT maps.

3.3. Future directions

There are a number of possible improvements that can be made to this approach. First, if 10-2 visual field data were available on a large group of healthy controls, then the visual field data could be referenced to the same continuous probability scale used for the OCT data. Second, summary statistics can be generated for the OCT maps analogous to the mean deviation, pattern standard deviation and glaucoma hemifield test of the visual field tests. In addition,

#143101 - $15.00 USD Received 25 Feb 2011; revised 28 Mar 2011; accepted 28 Mar 2011; published 5 Apr 2011

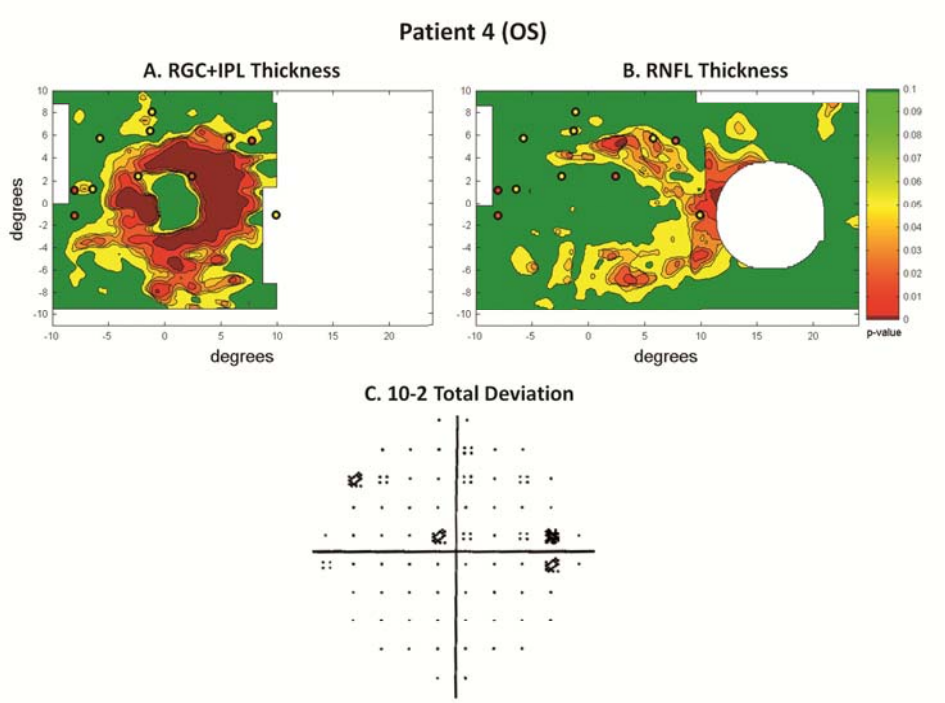

Fig. 6. Results for patient 4. A.B. Combined OCT/10-2 probability maps. C. 10-2 Total Deviation map.

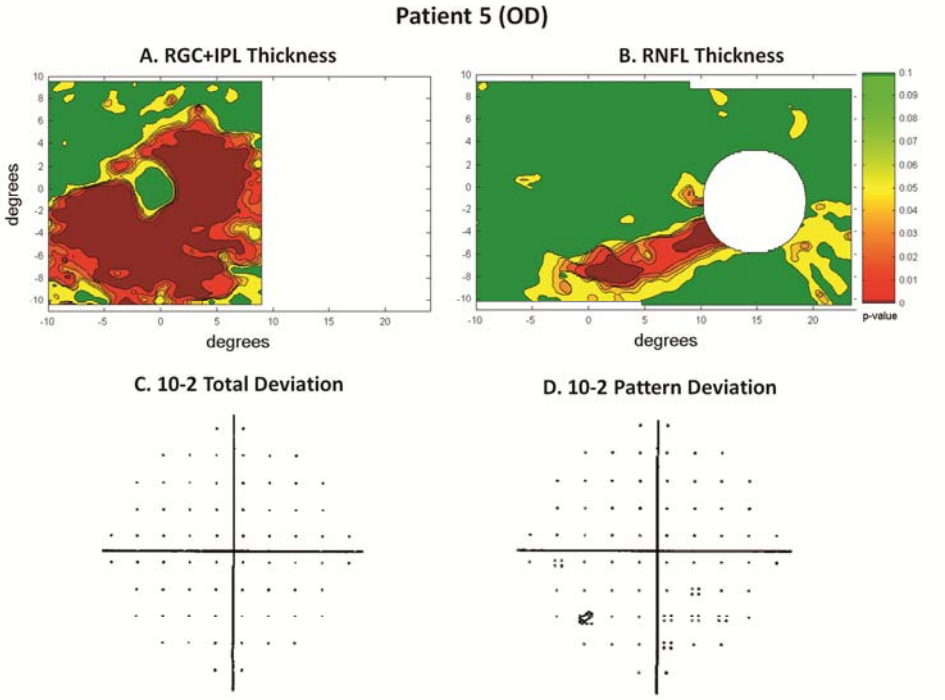

Fig. 7. Results for patient 5. A, B. Combined OCT/10-2 probability maps. C. 10-2 Total Deviation map. D. 10-2 Pattern Deviation map.

#143101 - $15.00 USD Received 25 Feb 2011; revised 28 Mar 2011; accepted 28 Mar 2011; published 5 Apr 2011

interocular comparisons could be obtained similar to those we have used in our multifocal visual evoked potential reports [11].

4. Conclusion

Combined visual field and OCT probability maps make it easy to compare structural and functional measures of glaucomatous damage. These combined maps should improve the diagnosis of glaucoma. Further, as the variance in OCT and visual fields measures should be independent, the visual field and OCT probabilities can be mathematically combined to improve the sensitivity/specificity of these tests.

Acknowledgments

This work was supported by NIH Grant EY-02115 and a grant of equipment from Topcon, Inc.

#143101 - $15.00 USD Received 25 Feb 2011; revised 28 Mar 2011; accepted 28 Mar 2011; published 5 Apr 2011